NASA TECHNICAL NOTE

NASA TN D-3771

NASA TN D-3771

A DESIGN STUDY OF A REGENERATIVELY COOLED NOZZLE FOR A TUNGSTEN WATER-MODERATED NUCLEAR ROCKET SYSTEM

by Richard L. Puthoff

Lewis Research Center

Cleveland, Ohio

NATIONAL AERONAUTICS AND SPACE ADMINISTRATION • WASHINGTON, D. C. • DECEMBER 1966

NASA TN D-3771

A DESIGN STUDY OF A REGENERATIVELY COOLED NOZZLE FOR A TUNGSTEN WATER-MODERATED NUCLEAR ROCKET SYSTEM

By Richard L. Puthoff

Lewis Research Center
Cleveland, Ohio

NATIONAL AERONAUTICS AND SPACE ADMINISTRATION

For sale by the Clearinghouse for Federal Scientific and Technical Information
Springfield, Virginia 22151 – Price $2.00

CONTENTS

A DESIGN STUDY OF A REGENERATIVELY COOLED NOZZLE FOR A TUNGSTEN WATER-MODERATED NUCLEAR ROCKET SYSTEM

by Richard L. Puthoff

Lewis Research Center

SUMMARY

A regeneratively cooled nozzle was used for the tungsten water-moderated nuclear rocket (TWMR). With hydrogen as the coolant, this type of nozzle provides a method for cooling the walls. In addition, it preheats the hydrogen to meet the rocket system heat exchanger and topping turbine requirements.

The design of a regeneratively cooled nozzle involves a computer program which calculates a heat balance at predetermined stations along the nozzle axis. These calculations are summed over the entire nozzle length providing an integrated nozzle coolant pressure drop and temperature increase.

To meet the design requirements set forth for the TWMR nozzle, a parametric study was conducted. In the case of nozzle parameters such as coolant tube areas, tube thicknesses, and number of coolant tubes, the effects of varying these parameters were felt most significantly by the nozzle ΔP_c (coolant pressure drop) with little effect on the ΔT_c (coolant temperature increase). Only when decreasing the inlet angle of the nozzle convergent section could a significant change in ΔT_c be effected. The tube stresses were also examined to determine the effect when varying these parameters.

The design selected was designated the TWMR reference design. At 100 percent rocket power, the reference design nozzle coolant pressure drop is 132.3 pounds per square inch, coolant temperature increase 119.2° R, and a maximum tube wall temperature of 1820° R. Nozzle performance calculations were also made at rocket reduced power conditions.

Although the nozzle design presented is unique to the TWMR rocket engine, the principles involved are applicable to other nuclear rocket designs.

INTRODUCTION

The current mode of propulsion for space vehicles has been through the use of chemical rocket engine systems. The requirements of some future space flights, however, are so demanding that chemical rocket performance becomes too limited. Nuclear rocket engines can achieve specific impulses much higher than the chemical systems. This results principally from utilizing hydrogen as a propellant for the nuclear rocket.

There has been, to date, considerable effort directed toward the development of a nuclear rocket engine system utilizing a graphite core reactor. This system is but one of several concepts which might be considered. One of the alternatives is a system employing a thermal reactor using uranium-tungsten dispersion as a fuel element material and water as a moderator.

A study of the feasibility of such a tungsten water-moderated nuclear rocket (TWMR) system was conducted at Lewis. In this study individual system components such as the reactor, pumps, nozzle, and so forth, were investigated as well as the characteristics of the overall system. As an aid in the program, a system reference design was used as a focal point for activity in a variety of disciplines.

The basic engine system (fig. 1) consists of a reactor, a hydrogen propellant feed system and a water-moderated circulating system, a water-to-hydrogen heat exchanger, and a thrust nozzle. Hydrogen is pumped from the storage tank through the system and

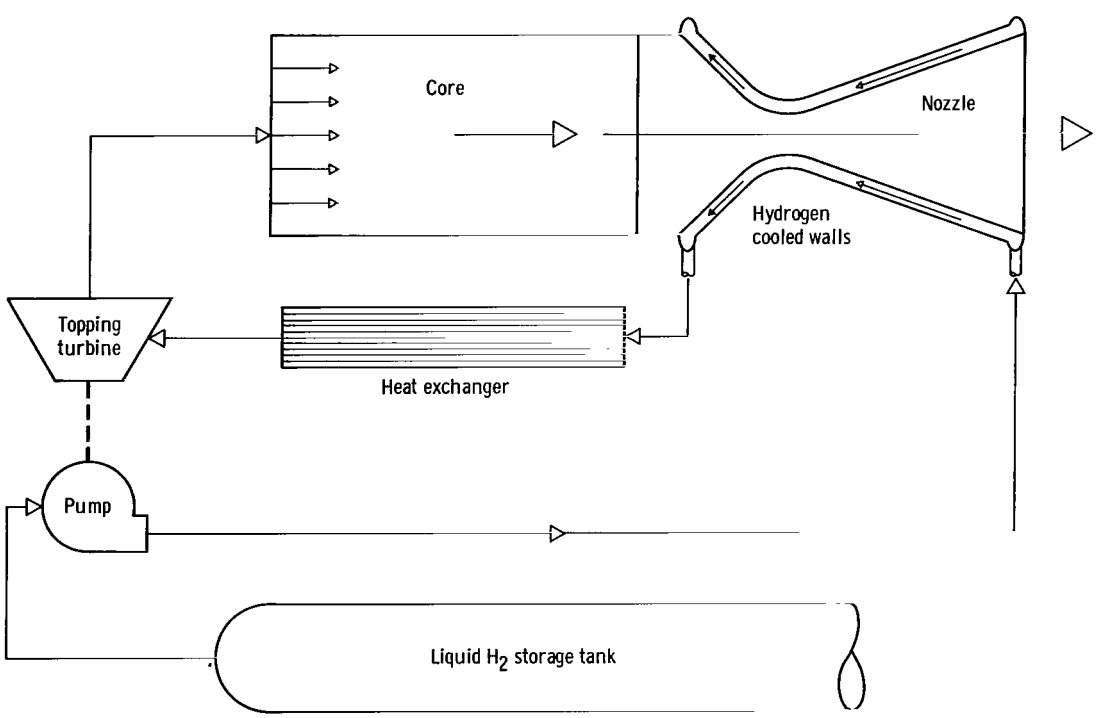

Figure 1. - TWMR propulsion system.

out the nozzle by the feed system. The nozzle is regeneratively cooled by propellant. After passing through the nozzle cooling passages, the hydrogen enters the heat exchanger where it removes heat from the water moderator. It then passes through a topping turbine to provide some or all of the pumping power before it enters the reactor core where it is heated by the fission energy. The gas leaves the core at high temperature and enters the nozzle where the energy is converted to thrust.

The use of a regeneratively cooled nozzle in the rocket propulsion system is dictated by the following considerations:

(1) High chamber gas temperatures

(2) The simplicity and efficiency resulting from using the propellant as a coolant

(3) The excellent heat transfer characteristics of hydrogen as a coolant

(4) The use of a topping turbine to provide some or all of the propellant pumping power requirements

(5) Increased hydrogen temperature entering the water moderator to hydrogen heat exchanger provides greater margin from freezing

The purpose of this report is to present the design study conducted on the nozzle component of the TWMR system reference design. This design has fixed the propellant mass flow, chamber pressure, and chamber temperature for the nozzle. In addition, certain design assumptions further restrict the choice of variables to define the nozzle. Therefore, within these overall restrictions calculations are made of nozzle performance as it is affected by the remaining parameters which are allowed to vary, namely, nozzle contour, coolant flow passage area, number of coolant tubes, and the wall thickness of the tubes. The nozzle performance was measured by the coolant pressure drop, temperature increase, and tube wall stresses.

The remainder of this report presents the results of the parametric studies of nozzle performance, a reference nozzle design for the TWMR and the off-design performance of this nozzle. Although there are many heat transfer and pressure drop correlations available, those selected and referenced herein are felt to be conservative for the design studied. This is in keeping with the underlying philosophy for the design of the TWMR system.

There is currently at Lewis a program for the investigation of heat transfer and pressure drop behavior of regeneratively cooled nozzles in which the basic mechanisms are receiving attention. The aims of that program are to improve calculational techniques by properly taking into account entrance effects, acceleration of gas on the hot gas side, cooling channel curvature and high wall-to-bulk temperature ratios on the cool gas side. References 1 to 3 report recent efforts.

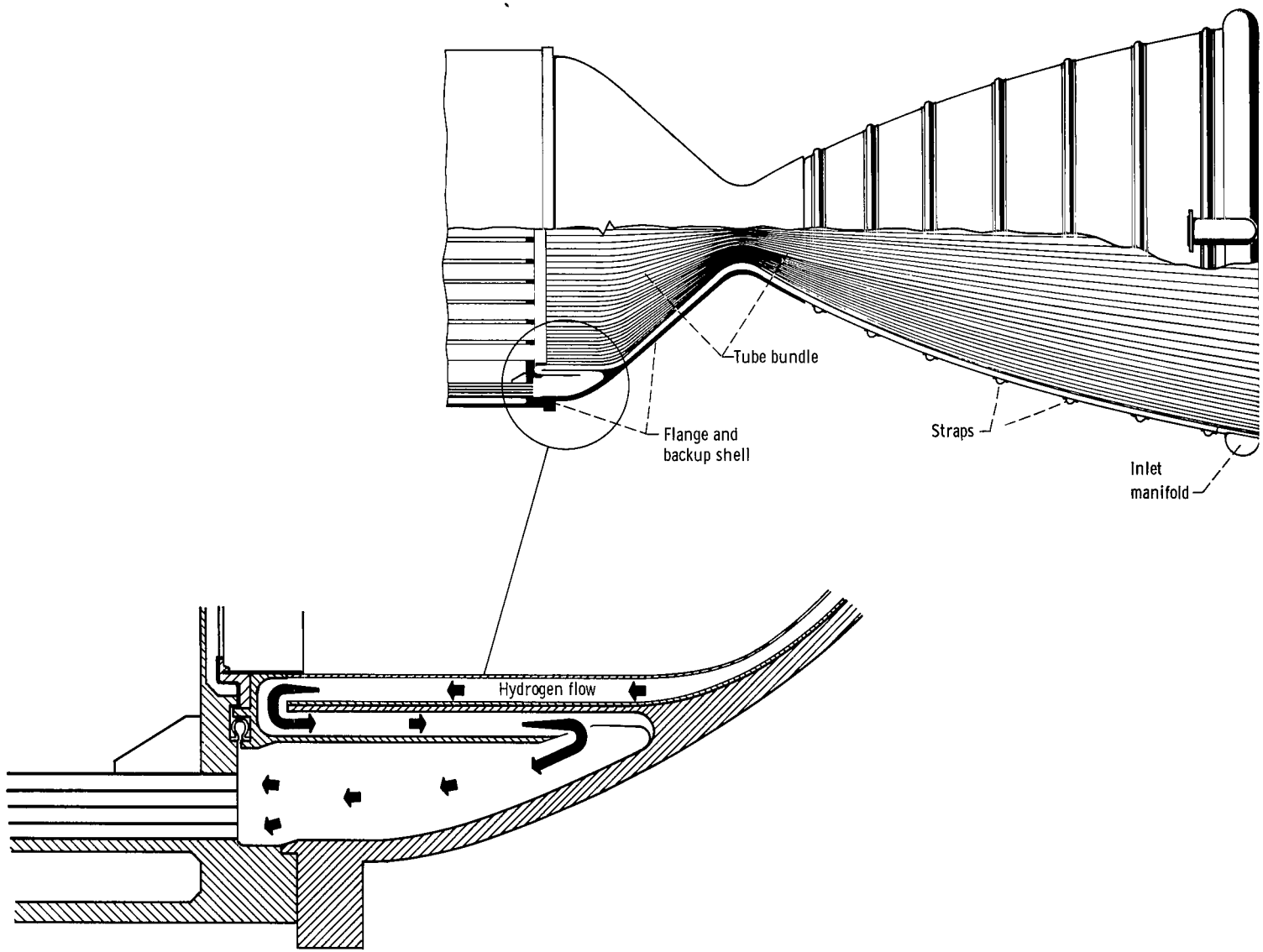

Figure 2. - TWMR nozzle.

TWMR HYDROGEN REGENERATIVELY COOLED NOZZLE

The design of the TWMR nozzle was based upon the general principles outlined previously. It consists of a flange and backup shell, tube bundle, and inlet manifold (see fig. 2). Fluid enters the tube bundle from the inlet manifold at the nozzle exit and counterflows with the hot gas to the nozzle inlet chamber. The tubes are supported structurally by the flange and backup shell in the high pressure chamber and throat regions and supported with hoop straps in the expansion section.

The design requirements of the nozzle were set forth along with certain assumptions which made the design calculations less rigorous but consistent with the goals of the study. An existing computer code was utilized along with recommendations from other groups at the Lewis Research Center who have designed similar size nozzles. The following is a discussion of these requirements, assumptions, and methods for the design of the TWMR nozzle.

Design Requirements and Objectives

Maximum heat gain in coolant bulk temperatures. - The TWMR reactor contains a heat exchanger for maintaining the water moderator at less than 240° F. The coolant for the heat exchanger is supplied by the hydrogen leaving the nozzle. To prevent icing in the heat exchanger, it is desirable to preheat the hydrogen as much as possible. In addition, the preheat added to the hydrogen increases the work available from the topping turbine. This first requirement is important since it is unique to the TWMR rocket concept.

Minimum pressure drop. - Any increase in heat is at a sacrifice in pressure drop. A pressure drop of 200 pounds per square inch was selected as a maximum allowable as dictated by the rocket system.

Temperature of wall not to exceed 2000° R. - The uncertainty of the calculations of tube wall stresses dictates 2000° R as a reasonably conservative design temperature. In addition, the material selected for the tubes was Inconel X, which demonstrates good strength characteristics at these elevated temperatures.

Maximum Mach number of 0.5 in coolant tubes. - This requirement is primarily to keep within pressure drop limitations.

Assumptions

The following assumptions define the full power operation of the nozzle, some of its geometry, and simplifying approximations used in the calculations:

(1) Chamber pressure P_{ch} = 600 pounds per square inch absolute, chamber temperature T_{ch} = 4460° R, W_G = 90.3 pounds per second, and W_C = 92.7 pounds per second. These values are a requirement of the system.

(2) Continuous tubes are used. Although some designs for regeneratively cooled nozzles are based on varying the number of coolant passages axially, such a technique was avoided in this case. From a fabrication point of view, a tube splice may be necessary to alleviate the high aspect ratios of the nozzle cross section at large nozzle area ratios.

(3) Formed tube configuration is used. This configuration allows the designer to vary the coolant flow area of the tubes without changing the number of tubes for maintaining the internal diameter of the tube bundle. Figure 3 is a sketch of the formed tube configuration. For design purposes, if the area of the tube is required to increase or decrease, as dictated by heat transfer calculations, only the b dimension need be increased or decreased. Consequently, the internal diameter of the tube bundle remains

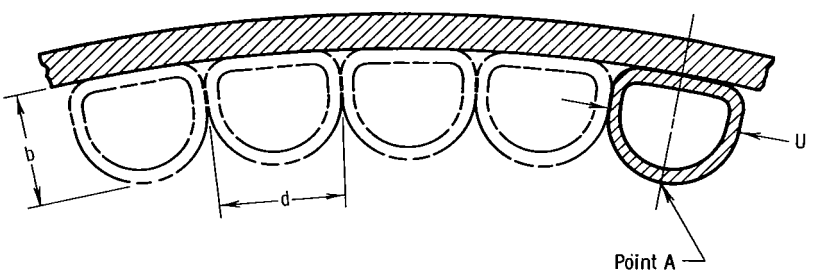

Figure 3. - Formed tube configuration.

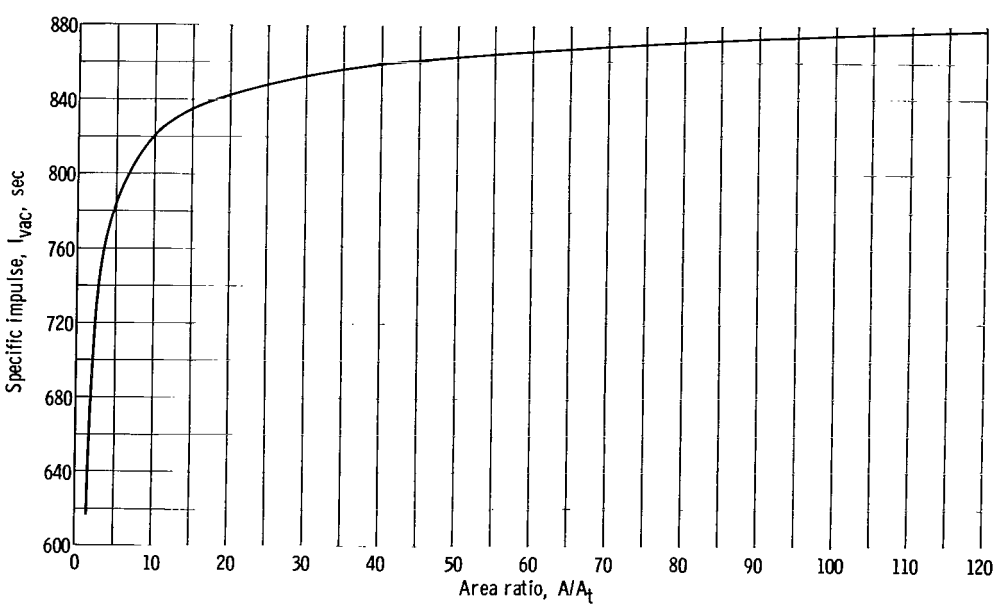

Figure 4. - Specific impulse plotted against nozzle area ratio. Chamber pressure, 600 pounds per square inch absolute; chamber temperature, 4460° R; propellant, hydrogen.

fixed by the contour yet the area of the tube can vary axially.

(4) The integrated heat flux is 1.25 times that computed for the pure circular inner-surface shapes (see fig. 3). This "ripple factor" accounts for the difference between the true area and the actual tube heat transfer area.

(5) Conduction across the wall neglects circumferential and axial conduction.

(6) No thermal barrier coatings on tubes are considered because maximum heat transfer to the coolant is desired.

(7) The area ratio of the regeneratively cooled section of the exit cone is 40 to 1. This study is primarily concerned with the heat transfer and pressure drop performance of the TWMR nozzle. The final area ratio used in the system will depend on a trade off between specific impulse and nozzle weight. Figure 4 shows the relationship of specific impulse of a nozzle exhausting to vacuum I_{vac} and the area ratio. Although the gain in specific impulse is decreasing with increasing area ratios as large ratios are reached, they may still be of interest for specific missions if the weight of the skirt is not excessive. For our purposes it is assumed that the area ratio will always be equal to or greater than 40 to 1 but that regenerative cooling will be used only out to area ratios of 40 to 1. This value is somewhat arbitrary and was based on the following two considerations:

(a) Cooling will probably not be required beyond this point.

(b) Diameters become so large that the ratio b/d (fig. 3) becomes unreasonable.

As will be pointed out later, the contour used in the heat transfer calculations is that for a 250 to 1 expansion ratio nozzle truncated at an area ratio of 40 to 1. For nozzles of different overall expansion ratios, the variations in contour out to the 40 to 1 ratio should not be significant.

(8) Throat area is 72 square inches. The propellant weight flow, chamber pressure, and chamber temperature are largely a requirement of the overall rocket system. To maintain these conditions, the nozzle throat area is calculated from the following expression:

$$A_t = \frac{W_G}{(144)P_{ch}\sqrt{\frac{g}{RT_{ch}}\gamma\left(\frac{2}{\gamma+1}\right)^{(\gamma+1)/(\gamma-1)}}} \qquad \text{(ref. 4)}$$

This equation is a simple isentropic expression assuming frozen flow and a constant γ. When using the computer program of reference 5, the characteristic velocity of the hydrogen is available as part of the output and the area can be calculated from the following expression:

$$A_t = \frac{C^* W_G}{(144) P_{ch} g} \qquad \text{(ref. 6)}$$

Design of the Hot Gas Nozzle Contour

Before the heat balance calculations for designing coolant tube passages are performed, the contour geometry of the nozzle, both inlet cone and exit cone, must be defined. The properties of the hot gas are then calculated and assigned to area ratios along the nozzle axis.

The primary objective of the nozzle contour design is to provide maximum efficiency at minimum length resulting in lighter nozzle weight. In the case of the convergent cone the design of the contour is not critical to nozzle efficiency. Generally, the subsonic contour is taken as a smooth curve such as a parabola or a straight line drawn in a smooth transition to the throat radius of curvature. The convergent angle can vary over a wide range within limitations dictated by nozzle length and stress.

The divergent cone design is more complex necessitating a careful selection to provide maximum overall nozzle efficiency and minimum nozzle weight. One consideration is whether the nozzle divergent cone is contoured or straight conical. The straight conical version provides a simple design easy to manufacture. The semidivergent angle of the cone, however, is limited to 15° (ref. 6) to avoid loss in nozzle efficiency. At higher area ratios, the 15° angle limitation results in excessively long and heavy nozzles. The contoured nozzle in comparison is a more sophisticated design providing parallel flow at the exit resulting in the highest nozzle efficiencies. In addition, the contoured design provides a shorter length and lighter weight nozzle compared to the straight conical nozzle.

Two methods are available for designing a contoured exit cone: a graphical method by Rao (ref. 7) and a method of characteristics (ref. 8). The graphical method is an approximate method and can define the contour of an optimum thrust nozzle by purely geometric means. The method of characteristics is an analytical method to define the optimum thrust contour. In the analytical method a characteristic net is constructed to define the expansion cone. Analyses differ as to their starting point of the characteristic net. The starting point may be taken at the sonic line which is considered to be straight and perpendicular to the throat, at the curved sonic line obtained by the method of Sauer (ref. 9), or at the source flow which is considered to be emanating from a point on the nozzle axis just upstream of the throat.

For the TWMR nozzle the basic exit cone contour was obtained from reference 10, figure 1. This is a bell-shaped contour obtained by the method of characteristics. The

characteristic net started at the curved sonic line obtained by the method of Sauer. The resultant length of the divergent section is 88 percent of the length of a 15° conical nozzle having an equal area ratio. As indicated previously, a 250 to 1 exit area ratio contour was determined and the shape out to an area ratio of 40 to 1 was used in the calculations.

The expansion of the hot gas through the nozzle requires that the isentropic properties of the gas be provided at incremental stations N along the nozzle axis for the subsequent heat transfer calculations. There are two alternatives for selecting these properties; assume the expansion process takes place without chemical changes (frozen flow) or assume the expansion process takes place everywhere in equilibrium (equilibrium flow) (ref. 11).

Frozen flow is the simpler case wherein it is assumed the specific heats of the exhaust gases are constant, that is, the gases are ideal and the flow variables depend only on the area variation of the nozzle according to the usual isentropic relationships. In the case of the TWMR nozzle the elevated temperatures (4500° R) of the exhaust gas cause dissociation. In computing the pressure, temperature, and gas velocity at any cross section of the nozzle, the energy released by changes in the composition must be accounted for. Therefore, the TWMR nozzle expansion process was considered as the more complex case (i.e., equilibrium flow).

A computer code (ref. 5) is available at Lewis which provides nozzle static temperatures and pressures at hydrogen equilibrium conditions for assigned chamber temperature, pressure, and area ratios. In addition, reference 12 provides the required property data for a wide range of temperature and pressures where hydrogen is dissociated.

This code is based on a one-dimensional flow model. For a bell-shaped contour, it is desirable to apply a correction factor to the one-dimensional data. This correction factor represents the ratio of the local mass velocity measured at the nozzle wall com-

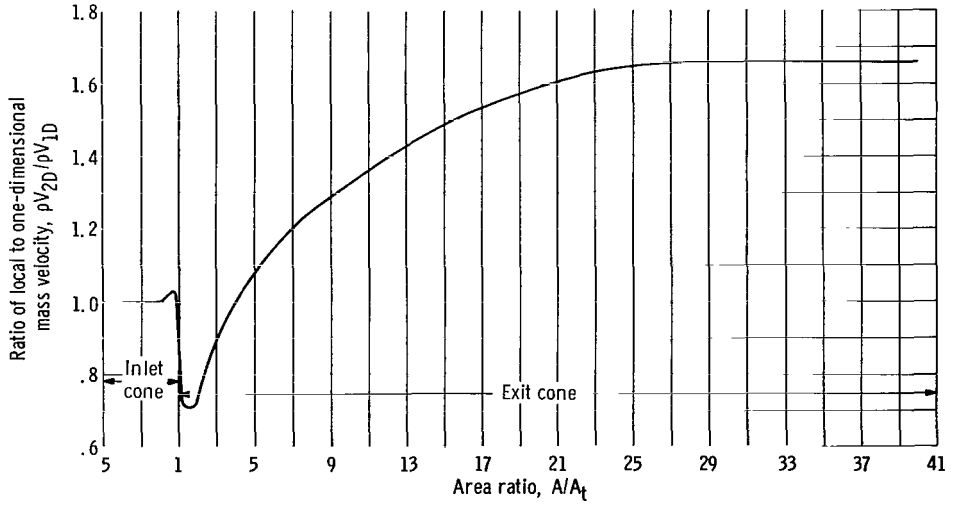

Figure 5. - Ratio of local to one-dimensional mass velocity.

pared with that predicted for one-dimensional flow. The corrections applied to the hydrogen mass flow and thermodynamic properties of the TWMR are shown in figure 5. The Jet Propulsion Laboratory also presents a curve similar to that in figure 5 in reference 13.

Heat Transfer and Pressure Drop in Coolant Passages

The design procedure for the heat transfer calculations is based upon the calculation of a balance between the heat flux on the hot gas side to the tube wall and the heat flux from the wall to the coolant. The procedure used is to match the heat flux on the hot gas side to the heat flux on the cold gas side resulting from a specified tube geometry. After the wall temperatures and heat fluxes are determined, the coolant pressure drop for a predetermined incremental length can be computed. These calculations are performed at intervals (stations) along the flow length of the nozzle commencing at the hot exhaust end.

The nozzle designed for the TWMR uses a computer code based on the aforementioned design procedures. Although there are many codes similar in approach, this code's main advantage is that the heat transfer coefficient in the high-velocity hot gas flow is based on enthalpies (refs. 14 and 15). This accounts not only for the variation of hydrogen properties with temperature in a wide range with an accuracy of better than 4 percent but also for dissociation of the hydrogen at high temperatures, where dissociation becomes appreciable. In this code, the heat transfer correlation on the hot gas side is

$$Nu_i = \mathscr{E}\, Re^{0.8}\, Pr^{0.333}$$

where $\mathscr{E}$ is defined in figure 6. This curve represents a conservative average of plots of unpublished data. The Nusselt number is

$$Nu_i = \frac{h_i C_p d}{K}$$

All transport properties of hydrogen for these equations are evaluated at a reference enthalpy defined as

$$i_{ref} = i_{GS} + 0.5(i_{GW} - i_{GS}) + 0.22\, Pr_{i,ref}^{0.33}(i_{GO} - i_{GS})$$

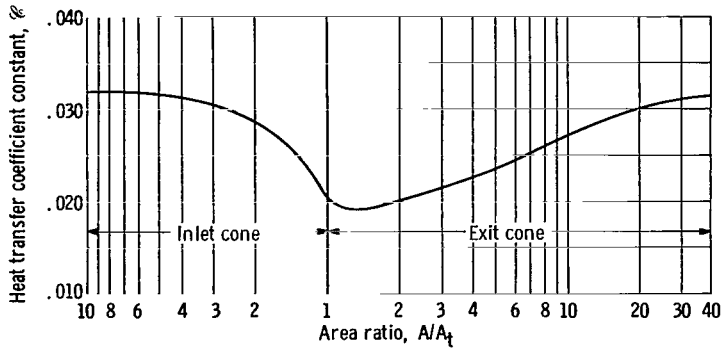

Figure 6. - Average $\mathscr{C}$ gas side distribution.

The heat transfer coefficient is

$$h_i = \frac{\mathscr{C}}{d^{1.8}} \left(\frac{4W_G \rho_{ref}}{\pi \rho_{GS}} \right)^{0.8} \frac{\mu_{ref}^{0.2}}{Pr_{ref}^{0.667}}$$

and the total heat flux q_G on the nozzle hot gas side becomes

$$q_G = h_i(i_{GA} - i_{GW})$$

where

$$i_{GA} = i_{GS} + Pr_{i,ref}^{0.33} (i_{GO} - i_{GS})$$

The evaluation of the heat flux carried away by the coolant q_C uses the heat transfer coefficient correlation of $Nu = 0.0208\ Re^{0.8}\ Pr^{0.4}\ c_2c_3$ where all transport properties are evaluated at the film conditions. A complete expression of the heat transfer coefficient becomes

$$h_C = \frac{0.0208}{d^{0.2}} \left(\frac{W_C \rho_{CF}}{A_C \rho_{CS} \mu_{CF}} \right)^{0.8} K_{CF} Pr_{CF}^{0.4} c_2 c_3$$

where

$$c_2 = \left[Re_{CF} \left(\frac{r_t}{r_c} \right)^2 \right]^{0.05} \quad \text{for} \quad Re_{CF} \left(\frac{r_t}{r_c} \right)^2 \geq 6.0$$

$$c_2 = 1.0 \text{ for } Re_{CF}\left(\frac{r_t}{r_c}\right)^2 < 6.0$$

and

$$c_3 = 1 + 0.01457 \frac{\mu_{CW}\rho_{CS}}{\mu_{CS}\rho_{CW}}$$

and the heat flux transferred to the coolant is

$$q_C = h_c(T_{CW} - T_{CS})$$

The pressure drop computed by the code consists of the friction pressure drop and the momentum pressure drop. It is calculated for each station on a per length basis. The pressure drop recorded is the average of the value at the N and N - 1 stations, multiplied by the incremental distance between them. The nozzle coolant ΔP_C is the summation of all stations.

For the friction pressure drop ΔP_f,

$$(\Delta P_f)_{N,N-1} = \frac{f}{(144)2g}\left(\frac{\rho_N + \rho_{N-1}}{d_N + d_{N-1}}\right)\left(V_{CS,N} + V_{CS,N-1}\right)^2 L_{N,N-1}$$

where

$$f = 4c_1\left(0.0014 + \frac{0.125}{Re_{CF}^{0.32}}\right)$$

and

$$c_1 = \left[Re_{CS}\left(\frac{r_t}{r_c}\right)^2\right]^{0.05} \text{ for } Re_{CS}\left(\frac{r_t}{r_c}\right)^2 \geq 6.0$$

$$c_1 = 1.0 \text{ for } Re_{CS}\left(\frac{r_t}{r_c}\right)^2 \leq 6.0$$

The total friction pressure drop is

$$\Delta P_f = \sum_{N=1}^{n} \Delta P_{f,N}$$

For the momentum pressure drop ΔP_m,

$$(\Delta P_m)_{N,N-1} = \frac{2W_C^2}{(144)g(A_{C,N} + A_{C,N-1})}\left(\frac{1}{\rho_N A_{C,N}} - \frac{1}{\rho_{N-1} A_{C,N-1}}\right)$$

The total momentum pressure drop is

$$\Delta P_m = \sum_{N=1}^{n} \Delta P_{m,N}$$

The coolant pressure drop ΔP_C is the algebraic sum of the friction and momentum pressure drops.

The computer code used for the design of the TWMR nozzle utilizes the equations listed previously to obtain a heat balance between the hot gas side heat flux and the coolant side heat flux. The nozzle is first divided into a number of stations. The dimensions of the coolant passages (area and hydraulic diameter), the isentropic equilibrium properties of the hot gas, and the initial thermodynamic properties of the hydrogen are assigned. The computer then performs the following basic tasks:

(1) Assumes a temperature for the tube wall exposed to the hot gases T_{GW}
(2) Calculates q_G
(3) Calculates the temperature drop through the wall
(4) Calculates q_C
(5) Compares q_G and q_C and assumes new T_{GW}
(6) Repeat steps (2), (3), and (4)
(7) Compares q_G with q_C for convergence - reiterates if necessary
(8) Evaluates coolant pressure drop

Stress Analysis in Coolant Tube Walls

When the nozzle design was satisfactory with regard to pressure drop and T_{GW}, the tube material stresses were calculated. The equations listed previously for determining

the temperature of the wall are valid for that surface exposed to the hot gases. The wall temperatures, however, reduce when progressing around the tube away from the hot gases resulting in a temperature gradient. A second temperature gradient occurs through the tube wall because of the large heat flux, which also varies circumferentially. These thermal stresses together with the usual shell structural stresses (membrane and bending) result in a complex stress situation.

In designing the TWMR nozzle the stress calculations were limited to an elastic analysis. The final design will require a more rigorous solution including a plastic flow analysis and internal heat generation.

The preliminary analysis was performed at the high heat flux station of the nozzle and on the tube wall where the maximum temperature occurs (see point A in fig. 3, p. 6). The stresses considered, in a plane normal to the tube axis, were bending and membrane due to diametrical load U, thermal due to a temperature gradient across the wall, and membrane due to pressure.

Longitudinal stresses were not calculated, but the effect of axial restraint of the tubes on their circumferential strain were considered.

The bending stress σ_B at point A in figure 3 is due to the diametrical load U. To determine the load U, the diametrical increase if the tube were unrestrained is calculated first. The diametrical increase in the tube because of the coolant pressure is

$$\delta_{\Delta P} = 2 \frac{(P_{CS} - P_{GS})r^2(1 - \nu^2)}{Et}$$

The diametrical growth due to the increase in metal temperature from room to operating temperature is

$$\delta_{\Delta T} = r\alpha\, \Delta T(1 + \nu)$$

where the average temperature of the tube wall is

$$\Delta T = \left(\frac{T_{GW} + T_{CW}}{2} - 530^{o}\,R\right)$$

These increases are offset by the hoop strain of the backup shell

$$\delta_S = -\left(2r \frac{1}{E} \sigma_S\right)$$

The total strain then is the algebraic summation in the hoop direction

$$\delta_{tot} = \delta_{\Delta P} + \delta_{\Delta T} + (-\delta_S)$$

Now if the tube is restrained on the diameter, a resultant load U occurs; that is,

$$U = \frac{\delta_{tot} E t^3}{(1 - \nu^2) r^3 \, 1.789}$$

The bending stress in the tube at point A of figure 3 and the nozzle station of maximum heat flux is

$$\sigma_B = \frac{1.092 \, Ur}{t^2}$$

and the membrane stress due to U at the point A is

$$\sigma_U = \frac{U}{2t}$$

The thermal stress due to the temperature gradient across the tube wall is

$$\sigma_{\theta B} = \frac{E\alpha(T_{GW} - T_{CW})}{2(1 - \nu)}$$

also the hoop stress due to the internal pressure is

$$\sigma_{\Delta P} = \frac{(P_{CS} - P_{GS})r}{t}$$

The total stress of the tube at point A of figure 3 and the nozzle station of maximum heat flux is the algebraic summation of the aforementioned stresses; that is,

$$\sigma_{tot} = \sigma_B + \sigma_{\theta B} + \sigma_{\Delta P} + \sigma_U$$

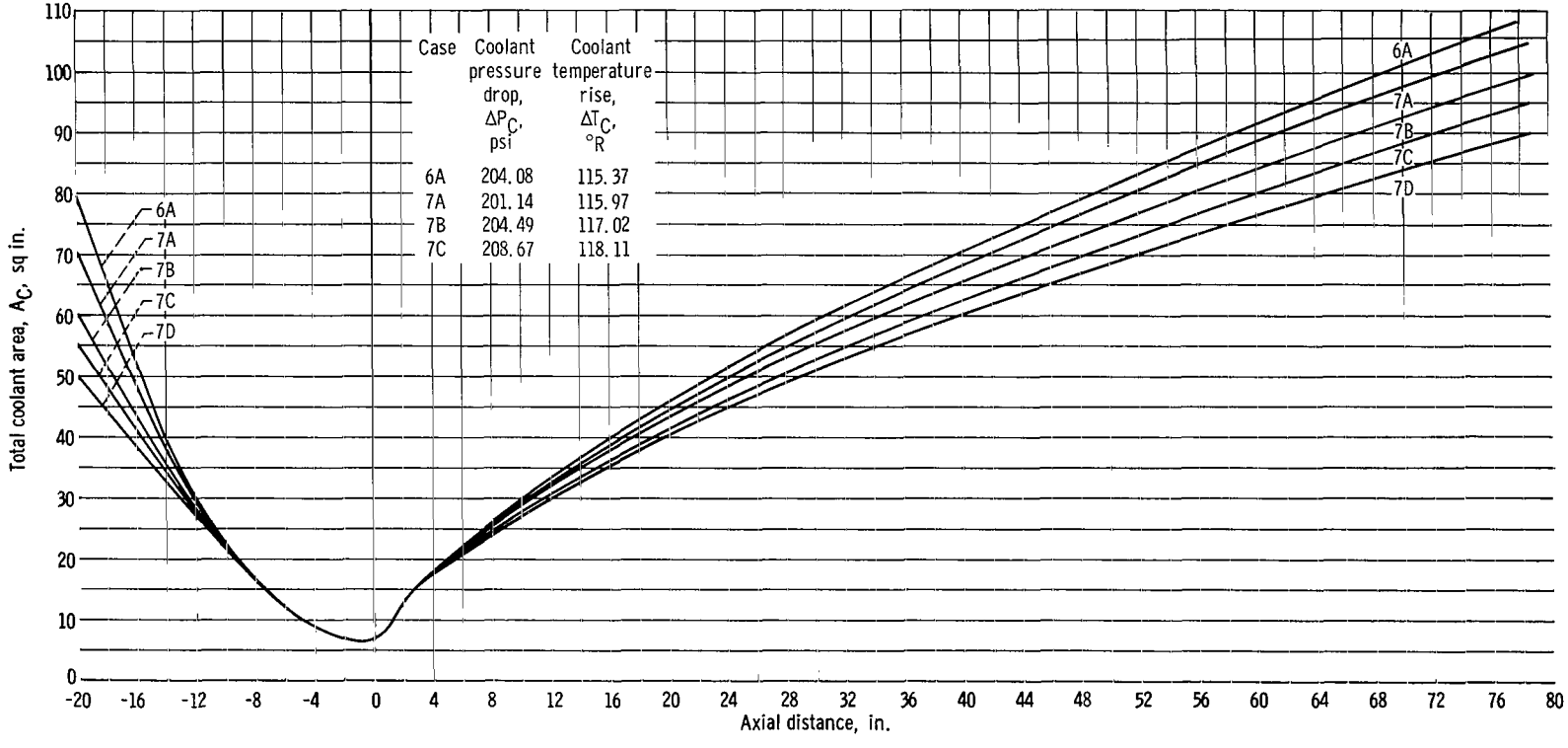

Figure 7. - Coolant area change in entrance and exit cone regions.

RESULTS

TWMR Nozzle Parametric Studies

Various nozzle configurations and input conditions were calculated on the computer. Each computer calculation was designated as a case. Output data included (but was not limited to) wall temperature on the hot gas side T_{GW}, wall temperature on the coolant side T_{CW}, total pressure of the coolant P_{CO} for each station and overall coolant temperature increase and pressure decrease as it passes through the entire length of the nozzle.

Effect of coolant flow area change on nozzle coolant performance. - In figure 7 the total flow area of the coolant tubes is plotted against the nozzle axial distance for five

TABLE I. - RELATIONSHIP OF STATION NUMBER AND NOZZLE AREA RATIO

Station number	Axial distance, in.	Area ratio, A/A_t	Station number	Axial distance, in.	Area ratio, A/A_t
1	0	40.00	25	77.83	1.00
2	8.14	35.97	26	78.09	1.02
3	18.38	30.53	27	78.34	1.03
4	28.70	24.79	28	78.59	1.04
5	39.37	18.91	29	78.85	1.06
6	50.12	12.31	30	79.11	1.08
7	61.05	6.57	31	79.37	1.13
8	66.59	4.24	32	79.64	1.17
9	72.27	2.22	33	79.91	1.22
10	73.44	1.86	34	80.20	1.26
11	74.03	1.69	35	80.50	1.34
12	74.31	1.62	36	80.82	1.41
13	74.597	1.52	37	81.17	1.51
14	74.88	1.44	38	81.52	1.64
15	75.18	1.36	39	81.86	1.78
16	75.47	1.29	40	82.86	2.16
17	75.76	1.22	41	83.62	2.69
18	76.03	1.17	42	84.56	3.26
19	76.30	1.13	43	86.49	4.64
20	76.56	1.10	44	88.58	6.46
21	76.82	1.06	45	90.47	8.28
22	77.08	1.04	46	92.50	10.54
23	77.33	1.03	47	94.45	12.94
24	77.58	1.02	48	96.40	15.60
			49	97.78	17.65

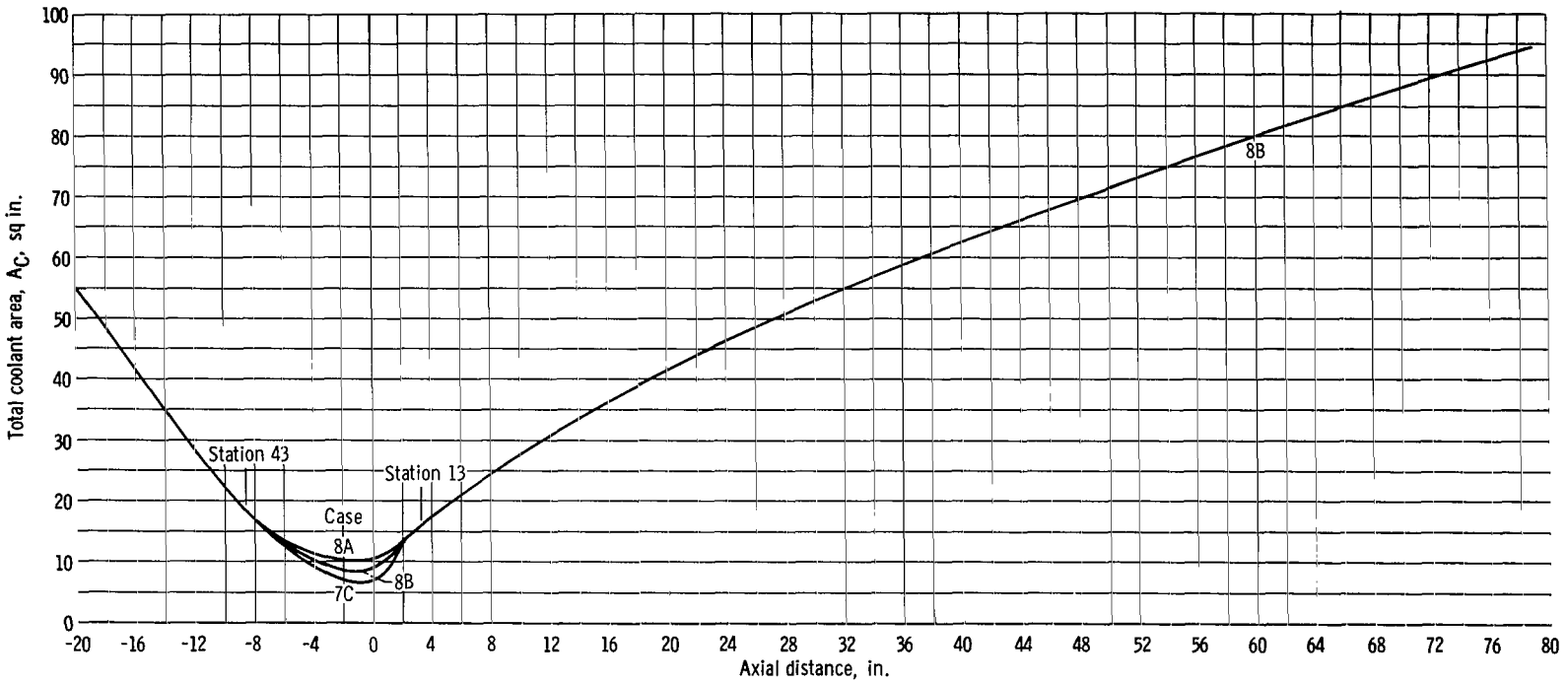

Figure 8. - Coolant area change in throat region.

different configurations. The variations were made, in each case, in the divergent cone from stations 1 to 13 and the entrance cone from stations 43 to 49. (See table I relating station number with nozzle axial distance and area ratio.) The primary objective was to determine the sensitivity of the integrated ΔT_C to these configuration changes. The ΔP_C and ΔT_C are listed in figure 7 for the corresponding cases. The significance of the coolant area changes between the aforementioned stations was so small that case 7D was not calculated. This is due primarily to the lower heat flux available at these stations.

The total coolant area was then changed for case 8 at the throat between stations 13 and 43 (see fig. 8). Two configurations are shown in figure 8 denoted as cases 8A and 8B. Also case 7C is shown for comparison. The result of a slight design change in this region is quite significant. Output data of cases 8A and 8B are presented in figure 9. Although the overall coolant ΔT_C remains fairly constant, the ΔP_C can be reduced from 132.3 to 97.4 pounds per square inch with only a 1.8° R difference in ΔT_C. More significant is the reduction in ΔP_C that is made between cases 7C and 8A, 208.7- and 97.4-pound-per-square-inch pressures at temperatures of $\Delta T_C = 118.1^{\circ}$ and 117.8°, respectively.

Table II tabulates the variables T_{GW}, M, ΔP_C, and ΔT_C for the cases discussed. Since the pressure drop is a function of the velocity squared, the data presented show that the coolant M is the significant factor for controlling the overall pressure drop. The values of M in the entrance and expansion sections are very small to begin with and changes in the coolant flow area result in an insignificant effect. The value of M in the throat region, however, is always the highest of the system and, in the case of the TWMR design, significant to begin with; therefore, design changes in this area can greatly affect the overall ΔP_C.

TABLE II. - EFFECT OF COOLANT LIQUID AREA CHANGE

Case	Maximum		Coolant pressure drop, ΔP_C, psi	Coolant temperature rise, ΔT_C, $^{\circ}R$	Liquid area change in section
	Hot gas wall temperature, T_{GW}, $^{\circ}R$	Mach number, M			
6A	1742.0	0.539	204.1	115.4	Convergent and exit cone
7A	1742	.510	201.1	116.0	Convergent and exit cone
7B	1741	.547	204.5	117.02	Convergent and exit cone
7C	1740	.555	208.7	118.1	Convergent and exit cone
8A	1860.4	.285	97.4	117.8	Throat
8B	1820	.366	132.3	119.2	Throat
21	2100	.180	55.5	117	Throat

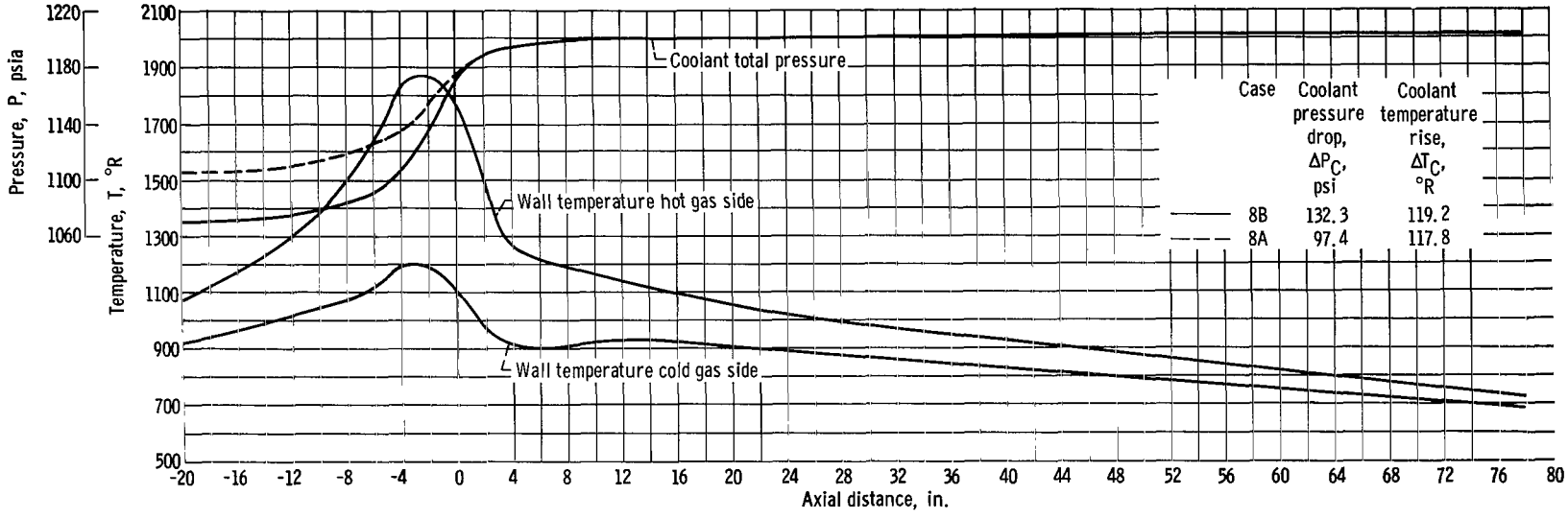

Figure 9. - Performance curves for cases 8A and 8B. Chamber pressure, 600 pounds per square inch absolute; chamber temperature, 4460° R; 100 percent power.

A calculation denoted as case 21 was performed in which the flow area was increased considerably above that of cases 8A and 8B. Again a significant reduction of ΔP_C is made (to 55.54 psi) with a small change in ΔT_C (to 117° R). The maximum M of 0.180 is well below the values for cases 7A and 7B (see table II). This improvement of the pressure drop, however, has resulted in an increase in the tube wall temperature T_{GW}. The reduction in the heat transfer coefficient on the cold gas side resulting from this low M in the throat area causes the wall temperature to exceed the design limit. This case demonstrates a design limit when the flow is being varied.

The optimum design ($\Delta T_{C,\,mas}$ at $\Delta P_{C,\,min}$) of the coolant flow area, therefore, becomes dependent on the allowable wall temperature of the tube on the hot gas side. Figure 10 shows T_{GW}, ΔP_C, and ΔT_C plotted against flow area. Data were taken from cases 7C, 8A, 8B, and 21.

Effect of number of coolant tubes on nozzle performance. - The variation in the number of coolant tubes as a useful parameter to control nozzle performance is limited. As the number of tubes is increased, the d dimension (fig. 3, p. 6) of the tube decreases. Fabrication costs and fluid flow considerations prevent the value of b/d from becoming too disproportionate. As the number of tubes is decreased and the d dimension increased, the tendency for longitudinal buckling increases. Therefore, the selection of the number of tubes must remain between the fabrication and stress analysis limits.

Figure 11 presents T_{GW}, ΔP_C, and ΔT_C plotted against the number of coolant tubes. When the number of coolant tubes is increased, M, ΔT_C, ΔP_C increases and T_{GW} decreases. For a change of 150 to 280 tubes, ΔP_C varies from 104 to 148 pounds per square inch, T_{GW} varies from 1819° to 1779° R, and ΔT_C varies from 116.7° to 119° R, respectively. This would be as expected since the change in the number of coolant tubes in effect changes the coolant area and the nozzle parameters behave as described in the previous section.

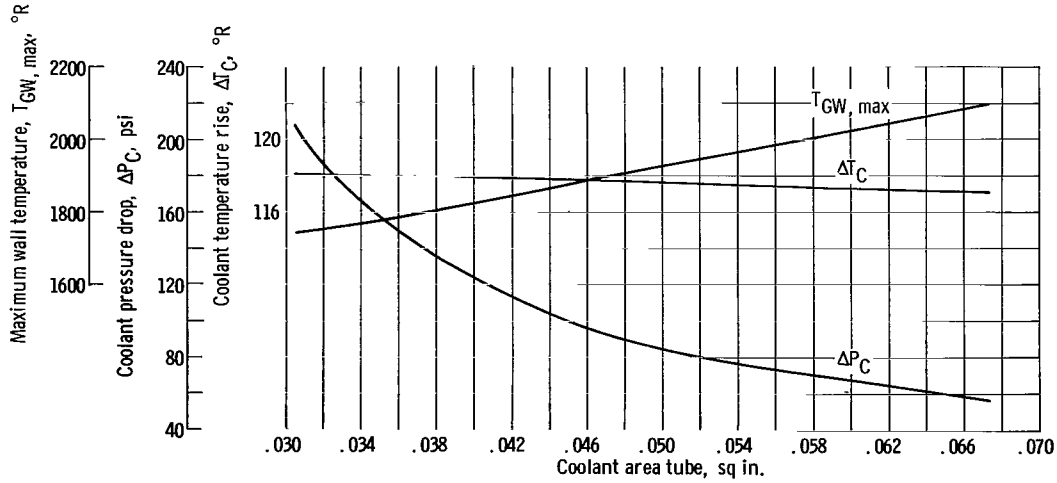

Figure 10. - Nozzle performance plotted against coolant area. Station 33.

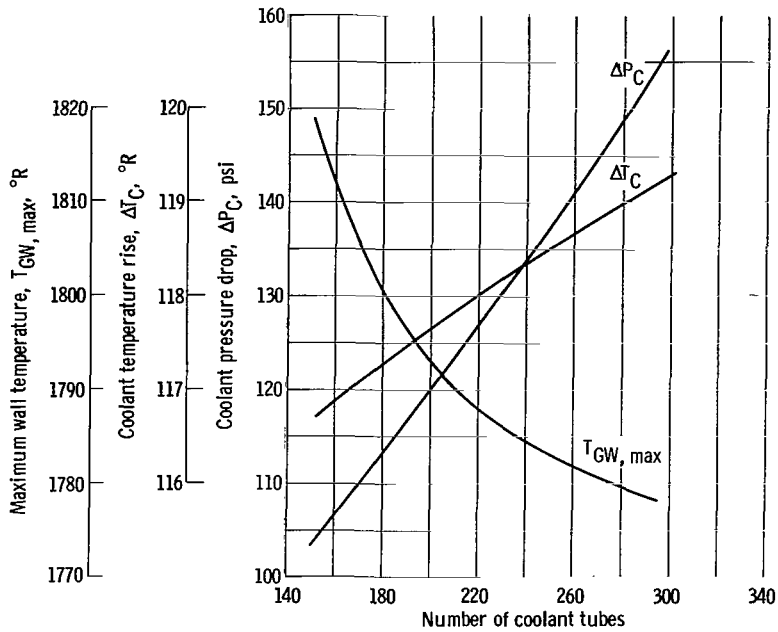

Figure 11. - Nozzle performance plotted against number of coolant tubes.

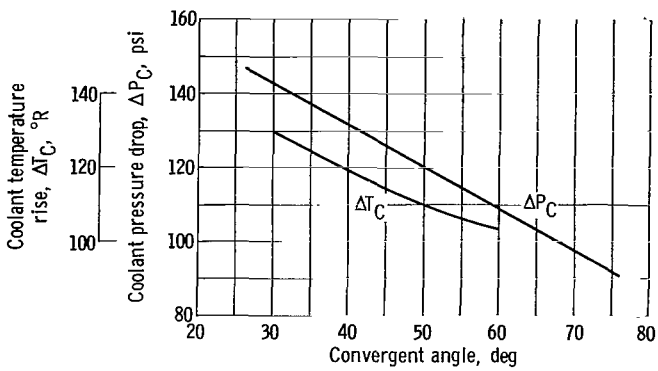

Figure 12. - Nozzle performance plotted against convergent angle. Case 8B.

Effect of inlet convergent angle on nozzle performance. - The convergent cone requirement of a regeneratively cooled nozzle for satisfying uniform hot gas streamline flow was previously outlined. Within these limitations the inlet angle was varied from 35° to 60° to determine its effect on the nozzle ΔT_C and ΔP_C. Figure 12 presents a plot of ΔT_C and ΔP_C as a function of the nozzle inlet convergent angle. Primarily because of the variation in coolant flow lengths, ΔP_C and ΔT_C vary inversely with nozzle inlet angle. The advantage for selecting a smaller inlet angle to gain ΔT_C is often overridden by limitations of ΔP_C. Large angles tend to increase stress problems.

Effect of coolant passage length on coolant temperature rise ΔT_C. - The coolant ΔT_C of the fluid is calculated from the equation $\Delta T = (q_G A / W_C C_p)$. Since the product $q_G A$ varies along the nozzle axis the total ΔT_C is an integrated value from the coolant inlet to the coolant exit.

Figure 13 is a plot of the rate of heat transferred per unit length Q/L as a function of the area ratio of the nozzle. The maximum value occurs sharply in the throat region and diminishes in the divergent skirt. Figure 13 emphasizes the small return for extend-

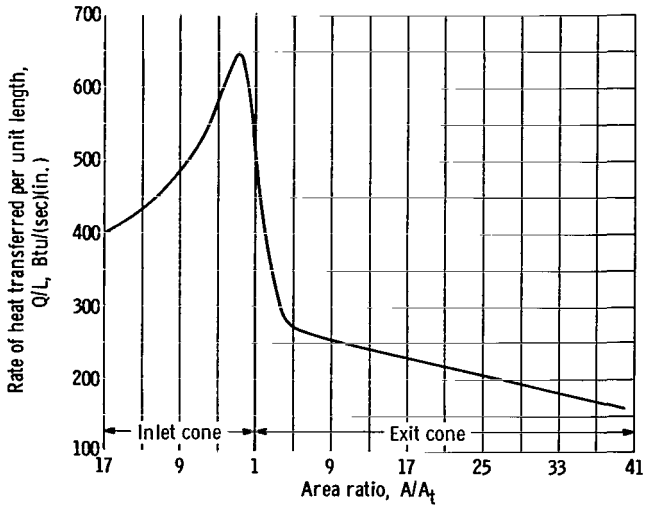

Figure 13. - Rate of heat transfered per unit length. Case 8B.

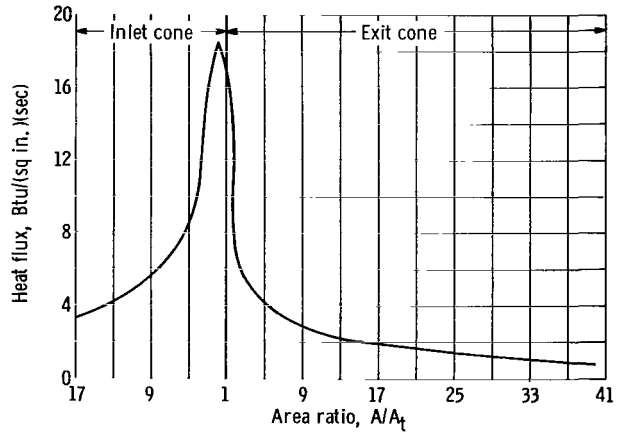

Figure 14. - Heat flux plotted against area ratio. Case 8B.

ing the regenerative section beyond a 40-to-1 area ratio in the exit cone.

Effect of heat transferred to tube from hot gas side q_G on tube stresses. - Although a high heat flux throughout the nozzle is desirable for optimizing the heat gain in the coolant, the temperature gradient across the tube wall due to these high fluxes results in large thermal stresses. Figure 14 shows a plot of the heat flux in the throat region. At these high fluxes the thermal stress can be reduced by decreasing the thickness of the tube walls. In this manner the temperature drop through the wall is controlled.

Figure 15 presents total tube stresses and ΔT_y plotted against tube wall thickness. The stress values plotted are composed of bending and membrane stresses in addition to the thermal stresses. Table III shows the breakdown of the total stress. There is little flexibility in varying the tube wall thickness. Dimensions of less than 0.006-inch thickness are difficult to manufacture and handle. Thicknesses greater than 0.012 inch may result in high thermal stresses. The stresses considered in this study would seem to indicate an advantage to using as thin a wall as is compatible with manufacturing techniques. It may be, however, that the longitudinal stresses causing a buckling tendency would require increasing wall thickness.

REFERENCE DESIGN PERFORMANCE

The nozzle design selected for the TWMR rocket was based on the parametric studies outlined. From these studies a specific nozzle configuration can be defined which will meet the requirements set forth in the section Design Requirements and Objectives. One

of the underlying aims of the reference design is a degree of conservativeness. Since the ΔT_C achievable in the nozzle coolant seemed independent of any of the parameters investigated, case 8B was chosen at the nozzle for use in the design. This represents a conservative (high) estimate of ΔP_C and a wall temperature below the 2000° R design limit.

The basic parameters of this design can be summarized as follows:

Chamber pressure at full power, psi	600
Chamber temperature at full power, $^{\circ}$R	4460
Coolant temperature rise ΔT, $^{\circ}$R	119.2
Coolant pressure drop ΔP, psi	132.3
Convergent cone angle, deg	40
Total flow area of coolant tubes	figure 8, case 8B
Number of coolant tubes	224
Tube wall thickness, in.	0.010
Maximum Mach number	0.37
Maximum tube stress, psi	76 130
Maximum wall temperature, $^{\circ}$R	1820
Nozzle material (tubes, backup shell, and flange)	Inconel-X

The performance of the reference design at 100 percent rocket power is plotted in figure 9 (case 8B, p. 20). Off-design power is achieved in the system by lowering the propellant flow. With the same nozzle configuration and chamber temperature, calculations were made to predict the performance at steady state operation for 60 and 37 percent rocket flow levels. These results are

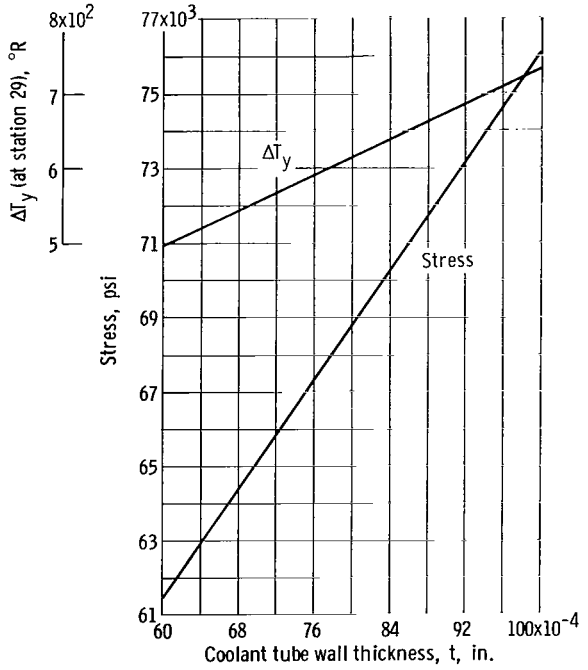

Figure 15. - Total tube stress and temperature gradient plotted against tube wall thickness.

TABLE III. - TENSILE STRESS AT INNER FIBER OF TUBE WALL

[Station 29.]

Stress, psi	Wall thickness, in.		
	0.010	0.008	0.006
Bending	-1.83×10^4	-1.410×10^4	-1.052×10^4
Thermal	9.22×10^4	7.95×10^4	6.65×10^4
Hoop	3.63×10^3	4.53×10^3	6.03×10^3
Membrane	-1.395×10^3	-1.08×10^3	$-.484 \times 10^3$
Total	76 130	68 850	61 526

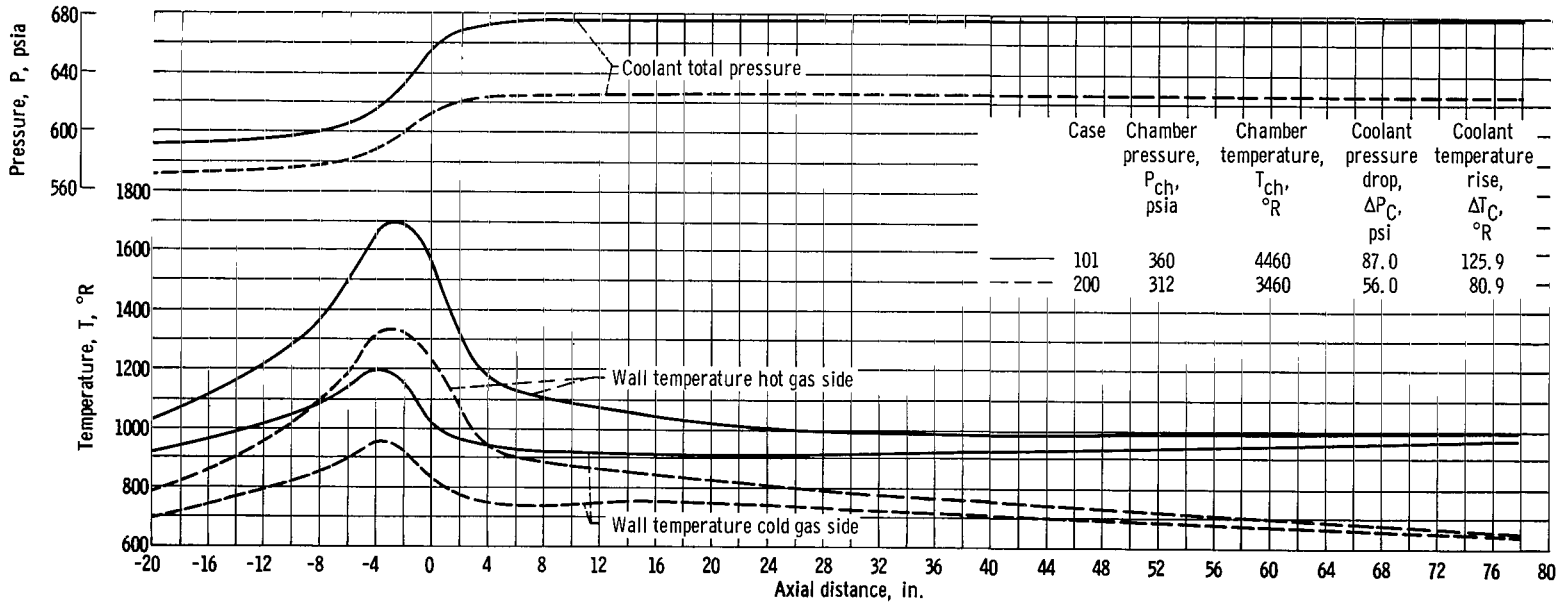

Figure 16. - Performance curves for cases 101 and 200 at 60 percent flow.

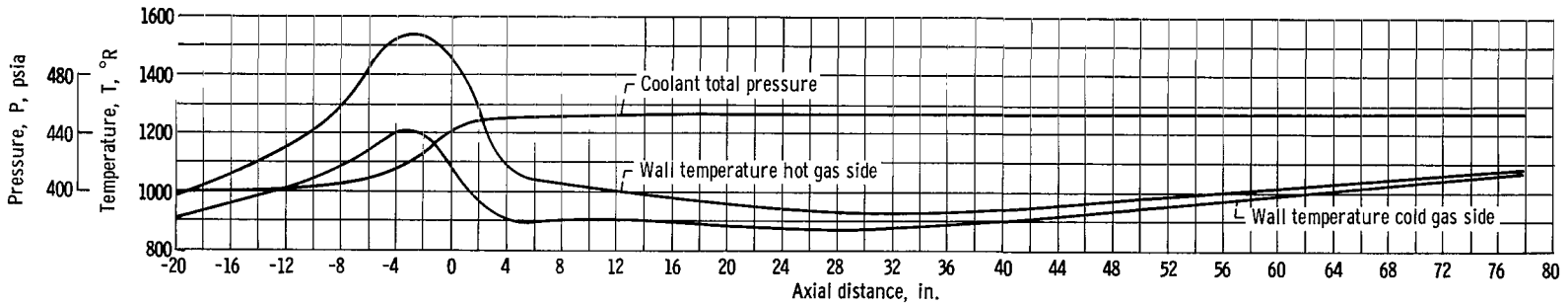

Figure 17. - Performance curves for case 302. Chamber pressure, 219.4 pounds per square inch absolute; chamber temperature, 4460° R; coolant pressure drop, 54.1 pounds per square inch; coolant temperature rise, 141.9° R; 37 percent flow.

TABLE IV. - OPERATING PERFORMANCE OF REFERENCE DESIGN AT VARIOUS POWER LEVELS

Case	Flow, percent	Nozzle chamber condition		Nozzle coolant tubes inlet condition		Density at throat, lb/cu ft	Coolant pressure drop, ΔP_C, psi	Coolant temperature rise, ΔT_C, ^oR	Propellant flow, lb/sec	
		Temperature, T_{ch}, ^oR	Pressure, P_{ch}, psia	Temperature, ^oR	Pressure, psia				Coolant, W_C	Hot gas, W_G
8B	100	4460	600	51.0	1203	1.87	132.3	119.2	92.7	90.3
101	60	4460	360	46.0	678.8	1.20	87.01	125.9	55.6	54.2
302	37	4460	219.4	44.8	454.6	.766	54.0	141.89	33.9	33
200	60	3460	312	44.2	627.5	1.79	56.0	80.9	55.6	54.2

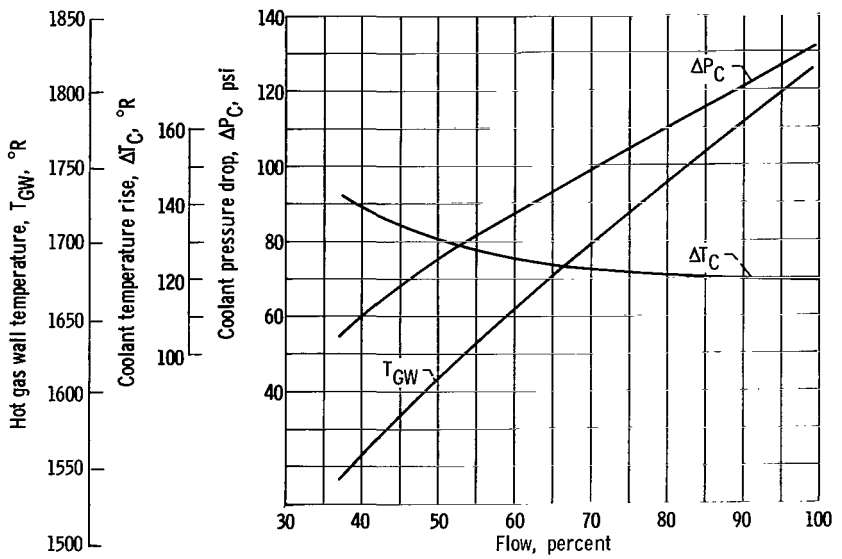

Figure 18. - Nozzle performance plotted against flow level. Chamber temperature 4460° R.

plotted in figures 16 and 17.

Also, table IV lists the performance parameters for both the full and reduced flow levels plotted in figures 9, 16, and 17. A fourth power level at 60 percent flow is presented which differs from the original 60 percent flow point in that the nozzle chamber temperature was lowered to 3460^o R.

The performance parameters of nozzle ΔP_C, ΔT_C, and maximum wall temperature were cross-plotted in figure 18 as a function of reactor flow level with a constant chamber inlet temperature of 4460^o R. Upon a close examination of these results, it becomes apparent that several nozzle design parameters are changing as the power level changes. These include the flow per unit area (at any particular station), heat transferred per unit weight flow, and density at the throat.

In the section Effect of Coolant Flow Area Change on Nozzle Performance, the

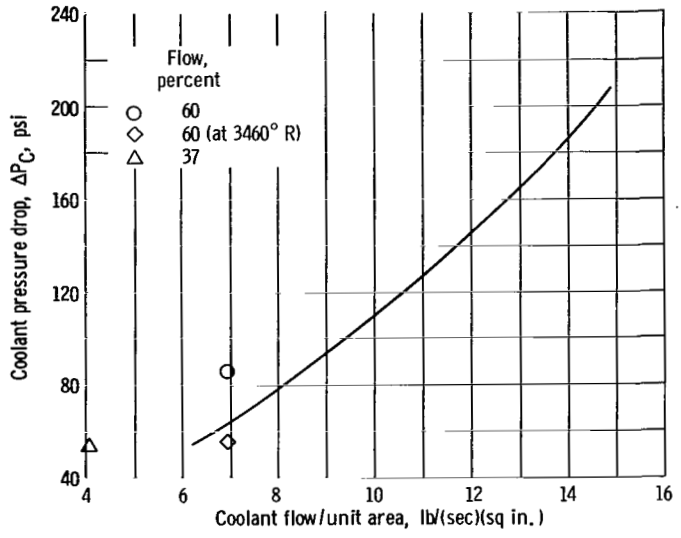

Figure 19. - Pressure drop plotted against coolant flow per unit area. Station 25.

importance of the coolant flow area design parameter was demonstrated. In these calculations the coolant weight flow and inlet coolant pressure and temperature were kept constant and changes from case to case were made in the coolant flow area which results in a change in the weight flow per unit of coolant area. Since the ΔT_C for all of these cases is practically constant, then the heat input per unit weight flow and subsequent coolant density at any given station due to heat addition is also nearly constant.

Figure 19 presents ΔP_C for the 100 percent power performance cases plotted against mass flow per unit area with station 25 as the reference area. With nearly the same density, the ΔP_C increase with increasing weight flow per unit area is almost a direct result of the coolant velocity increase. Also plotted in figure 19 are the points representing the reduced power performance of the reference design. The 60 and 37 percent power conditions have ΔP_C points that fall above the curve since their heat transfer per unit weight flow increases as reflected in their ΔT_C (see table IV) and their subsequent coolant density decreases at the throat (station 25). Conversely, the 46.5 percent power condition whose chamber temperature is reduced to 3460° R has a ΔP_C point which falls below the curve due to the increase in the coolant density at the throat.

CONCLUSIONS

One of the prime aims of the nozzle design for the tungsten water-moderated nuclear rocket system is the maximum addition of heat to the coolant while reasonable pressure drops and wall temperatures are maintained. An effective method found for increasing the heat transferred into the coolant is decreasing the angle of the convergent section of the nozzle thereby increasing heat transfer area in regions of reasonably high heat flux. This technique has the disadvantages of increasing pressure drop significantly and increasing the weight and length of the nozzle assembly.

A more significant parameter in the design is the total area of the coolant flow tubes in the region of the throat. Although it has little effect on the heat transferred to the coolant, the pressure drop is quite sensitive to this factor. As coolant flow area is

increased, pressure drop decreases and system topping turbine operation is improved. This improvement is accompanied by an increase in wall temperature so that the allowable wall temperature becomes the limit to this method of decreasing pressure drop.

Attempts to gain more heat by increasing the cooled length of the exit nozzle result in insignificant improvements.

Tube thicknesses should be kept as small as is consistent with fabrication techniques and thereby reduce thermal stresses due to temperature gradients across the wall.

A reference nozzle design with conservative coolant performance was chosen for the tungsten water-moderated nuclear rocket system with the following characteristics at normal operating conditions:

Chamber pressure at full power P_{ch}, psi	600
Chamber temperature at full power T_{ch}, ^{o}R	4460
Coolant temperature rise ΔT_C, ^{o}R	119.2
Coolant pressure drop ΔP_C, psi	132.3
Maximum Mach number in coolant tubes	0.37
Total tube stress (maximum), psi	76 130
Maximum wall temperature $T_{GW, max}$, ^{o}R	1820

Calculations at several off-design operating conditions indicate no overtemperature tendencies in the tube walls. The pressure drop and temperature increase behavior at these conditions depend on the variation of the coolant weight flow and temperature of the hot gas into the nozzle chamber.

Lewis Research Center,
National Aeronautics and Space Administration,
Cleveland, Ohio, August 15, 1966,
122-28-02-04-22.

APPENDIX - SYMBOLS

A	area, sq ft
C^*	characteristic velocity, ft/sec
C_p	specific heat at constant pressure, Btu/(lb)(^oR)
$\mathscr{C}$	constant in hot gas heat transfer equation
c_1	correction for friction factor
c_2, c_3	correction factor for heat transfer coefficient
d	hydraulic diameter, ft
E	modulus of elasticity, psi
f	friction factor
g	gravitational constant, ft/sec^2
h_C	tube surface heat transfer coefficient (cold gas), Btu/(sq ft)(sec)(^oR)
h_i	tube surface heat transfer coefficient (hot gas), lb/(sq ft)(sec)
I_{vac}	specific impulse of nozzle exhausting to vacuum
i	enthalpy, Btu/lb
K	thermal conductivity, Btu/(ft)(sec)(^oR)
L	fluid flow length, in.
M	Mach number
N	station number
Nu	Nusselt number
n	number of stations
P	pressure
ΔP_C	coolant pressure drop, $\Delta P_f + \Delta P_m$, psi
ΔP_f	friction pressure drop, psi
ΔP_m	momentum pressure drop, psi
Pr	Prandtl number
Q	total heat transferred, Btu/(sec)
q_C	heat transferred from tube to fluid on coolant side, Btu/(sq ft)(sec)
q_G	heat transferred to tube from hot gas side, Btu/(sq ft)(sec)
R	gas constant, ft-lb/(lb)(^oR)
Re	Reynolds number
r	radius, in.
r_t/r_c	ratio of tube radius to radius of curvature
T	temperature, ^oR
ΔT_C	coolant temperature rise, ^oR
ΔT_y	$T_{GW} - T_{CW}$, ^oR
t	coolant tube wall thickness, in.
U	diametrical load, lb
V	velocity, ft/sec
W	mass flow, lb/sec
α	thermal coefficient of linear expansion, in./(in.)(^oR)
γ	ratio of specific heats
$\delta_{\Delta P}$	diametrical increase (pressure), in.
δ_S	diametrical increase (hoop), in.

$\delta_{\Delta T}$	diametrical increase (temperature), in.
μ	absolute viscosity, lb/(ft)(sec)
ν	Poisson's ratio
ρ	density, lb/cu ft
ρV_{1D}	one-dimensional mass velocity, lb/(sq ft)(sec)
ρV_{2D}	local mass velocity, lb/(sq ft)(sec)
σ_B	bending stress, psi
$\sigma_{\Delta P}$	hoop stress, psi
σ_S	hoop stress backup shell, psi
σ_U	membrane stress, psi
$\sigma_{\theta B}$	thermal stress, psi

Subscripts:

C	coolant bulk total
CF	coolant film
ch	chamber
CO	coolant bulk total
CS	coolant bulk static
CW	coolant wall
G	gas
GA	recovery hot gas bulk
GO	hot gas total
GS	hot gas bulk static
GW	hot gas wall
i	variable based on enthalpy
max	maximum
min	minimum
ref	reference film
t	throat
tot	total
W	wall

REFERENCES

1. Boldman, Donald R.; Schmidt, James F.; and Fortini, Anthony: Turbulence, Heat-Transfer, and Boundary Layer Measurements in a Conical Nozzle with a Controlled Inlet Velocity Profile. NASA TN D-3221, 1966.

2. Schacht, Ralph L.; Quentmeyer, Richard J.; and Jones, William L.: Experimental Investigation of Hot-Gas Side Heat-Transfer Rates for a Hydrogen-Oxygen Rocket. NASA TN D-2832, 1965.

3. Miller, John V.; and Taylor, Maynard F.: Improved Method of Predicting Surface Temperatures in Hydrogen-Cooled Nuclear Rocket Reactor at High Surface-to Bulk-Temperature Ratios. NASA TN D-2594, 1965.

4. Shapiro, Ascher H.: The Dynamics and Thermodynamics of Compressible Fluid Flow. Ronald Press Co., 1953.

5. Gordon, Sanford; Zeleznik, Frank J.; and Huff, Vearl N.: A General Method for Automatic Computation of Equilibrium Compositions and Theoretical Rocket Performance of Propellants. NASA TN D-132, 1959.

6. Zucrow, Maurice J.: Aircraft and Missile Propulsion. John Wiley and Sons, Inc., vols. 1 and 2, 1958.

7. Rao, G. V. R.: Approximation of Optimum Thrust Nozzle Contour. ARS J., vol. 30, no. 6, June 1960, p. 561.

8. Sauer, R.: Method of Characteristics for Three-Dimensional Axially Symmetric Supersonic Flows. NACA TM-1133, 1947.

9. Sauer, R.: General Characteristics of the Flow through Nozzles at Near Critical Speeds. NACA TM-1147, 1947.

10. Neumann, Harvey E.; and Bettinger, Paula J.: A Comparative Analysis of Convective Heat Transfer in a Nuclear Rocket Nozzle. TN D-1742, 1963.

11. Cronvich, Lester L.; and Faro, Ione D. V., eds.: Ducts, Nozzles and Diffusers. Vol. 6, sect. 17 of Handbook of Supersonic Aerodynamics. Rep. No. 1488, Bureau of Naval Weapons, Jan. 1964.

12. Grier, Norman T.: Calculation of Transport Properties and Heat-Transfer Parameter of Disassociating Hydrogen. NASA TN D-1406, 1962.

13. Back, L. H.; Massier, P. F.; and Gier, H. L.: Convective Heat Transfer in a Convergent-Divergent Nozzle. Tech. Rep. No. 32-415, Rev. 1 (NASA CR-57326), Calif. Inst. Tech., Jet Prop. Lab., Feb. 15, 1965.

14. Eckert, Ernst R. G.; and Drake, Robert M., Jr.: Heat and Mass Transfer. Second ed., McGraw-Hill Book Co., Inc., 1959.

15. Benser, W. A.; and Graham, R. W.: Hydrogen Convective Cooling of Rocket Nozzles. Paper No. 62-AV-22, ASME, 1962.

16. Hess, H. L.; and Kunz, H. R.: A Study of Forced Convection Heat Transfer to Supercrticial Hydrogen. J. Heat Transfer, vol. 87, no. 1, Feb. 1965, pp. 41-48.

17. Timoshenko, S.; and Goodier, J. N.: Theory of Elasticity. Second ed., McGraw-Hill Book Co., Inc., 1951.

18. Roark, Raymond J.: Formulas for Stress and Strain. Third ed., McGraw-Hill Book Co., Inc., 1954.

"The aeronautical and space activities of the United States shall be conducted so as to contribute . . . to the expansion of human knowledge of phenomena in the atmosphere and space. The Administration shall provide for the widest practicable and appropriate dissemination of information concerning its activities and the results thereof."

—NATIONAL AERONAUTICS AND SPACE ACT OF 1958

NASA SCIENTIFIC AND TECHNICAL PUBLICATIONS

TECHNICAL REPORTS: Scientific and technical information considered important, complete, and a lasting contribution to existing knowledge.

TECHNICAL NOTES: Information less broad in scope but nevertheless of importance as a contribution to existing knowledge.

TECHNICAL MEMORANDUMS: Information receiving limited distribution because of preliminary data, security classification, or other reasons.

CONTRACTOR REPORTS: Technical information generated in connection with a NASA contract or grant and released under NASA auspices.

TECHNICAL TRANSLATIONS: Information published in a foreign language considered to merit NASA distribution in English.

TECHNICAL REPRINTS: Information derived from NASA activities and initially published in the form of journal articles.

SPECIAL PUBLICATIONS: Information derived from or of value to NASA activities but not necessarily reporting the results of individual NASA-programmed scientific efforts. Publications include conference proceedings, monographs, data compilations, handbooks, sourcebooks, and special bibliographies.

Details on the availability of these publications may be obtained from:

SCIENTIFIC AND TECHNICAL INFORMATION DIVISION

NATIONAL AERONAUTICS AND SPACE ADMINISTRATION

Washington, D.C. 20546